Spiking Neuron Model for Wavelet Encoding of Temporal Signals

Zhenzhong Wang, Lilin Guo, and Malek Adjouadi
Center for Advanced Technology and Education, Florida International University, Miami, FL, USA

Abstract – *Wavelet decomposition is a widely used method to preprocess temporal signals before they could be analyzed by Artificial Spiking Neural Networks (ASNN). This study proposes a biological plausible way to encode the temporal signals into spike trains with wavelet amplitude spectrum represented by the delay phases during each encoding period. The encoding method is presented in the form of a spiking neuron model for easy implementation in ASNN. The proposed neuron model is tested on encoding of human voice records for speech recognition purpose, and compared with results from continuous wavelet transform. The nonlinearity properties and choices of biological plausible wavelet kernels for the proposed encoding method is discussed for the generality of its application.*

Keywords: Phase encoding, Spiking neural network, Wavelet decomposition, Leaky Integrate-and-Fire neuron

1 Introduction

The most significant difference between Artificial Spiking Neural Networks (ASNN) and traditional neural networks is that information in ASNN is represented by spike trains which are a series of pulses with timings of interests. There are mainly two kinds of interpretations developed in signal processing applications about how information is related to spike trains: (1) the rate encoding, which assumes that the information is encoded by the counts of spikes in a short time window; and (2) the spike time encoding which considers information carried at the exact time of each pulse in the spike train. Although the mechanisms for data representation and analysis using biologically-inspired neural networks is still under development, empirical evidence has shown that spike time encoding might be more reliable in explaining experiments on the biology of nervous systems[1], [2].

Both rate encoding and spike time encoding essential in ASNN applications. The easiest way to rate encode an analog signal is to feed it to a Poisson neuron, which fires output spikes at probability proportional to its membrane potential, thus making its firing rate within a short time window proportional to the amplitude of the input signal. Such an encoding method has been adopted by Sprekeler *et al*. [3]. and Keer *et al*. [4] in order to analyze the recurrent ASNN behaviors. Although Poisson neuron model is simple and suitable for theoretical analysis, it was rarely implemented in real-world applications due to its inaccuracy in mapping analog signals to spike trains. De Garis *et al*. [5] introduced another rate encoding method which deconvolves the input signal into its individual spike responses, so that the post-synaptic potential of the encoded spike train could be quite similar to the original signal. Schrauwen and Van Campenhout [6] improved algorithm proposed by De Garis *et al*. by optimizing the deconvolution threshold yielding the so-called Bens Spiker Algorithm (BSA). BSA has been used widely as a rate encoding method for ASNN applications [7]–[9]. The major problem of this type of rate encoding is that an averaging time window is required for each sampling of the input signal, which as a consequence limits the temporal resolution of the encoded signals.

Synchronized spike time encoding, dubbed as Phase Encoding (PE), was also widely used in ASNN application. A simple implementation of PE could be realized by linearly mapping the input signal to the delay of spikes within each synchronizing period [10]. This implementation of PE requires the input signal either to be static or vary at frequencies much lower than the synchronizing frequency. Temporal receptive fields could also be utilized for PE to improve the encoding resolution [11], [12]. To be more biologically plausible, Rumbell *et al*. [13] introduced a synchronizing method which considered spiking neurons as PE units instead of performing linear mapping between analog values and spike delays. Receptive fields in this study were applied to the amplitude dimension instead of the temporal dimension, which yielded good performance for static input data. However, PE method which could accurately encode temporal signals is still under development.

In this paper, we propose a preprocessing unit for the Leaky Integrate-and-Fire (LIF) spiking neurons. The assumption is that a neuron model combining the preprocessing unit with a LIF neuron could be used to encode analog signals with wide frequency range. We will demonstrate that our preprocessing unit could decompose the input signal into wavelet spectrum, and further encode the spectrum amplitude into the delay amount between output spikes and the clock signals. Empirical results of PE encoding of speech records are provided, with linearity, temporal

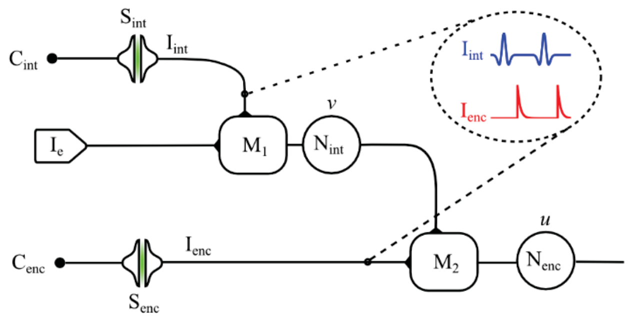

Fig. 1: Structure of the Two-Stage Modulate-and-Integrate Module

resolution issues and possible extension of the encoding method discussed.

2 Encoding Neuron Model

In this section, we will demonstrate that an array of specially designed LIF neurons could perform wavelet decomposition of temporal signals. This special design of a LIF neuron differs from traditional LIF neurons by incorporating a two-stage spike triggered modulate-and-integrate module to pre-process the input signal. Such design was inspired by the multiplication relationship found among afferent synaptic currents in biological neurons [14]. Delay synchronized spikes sent to the two synapses integrated in the special designed LIF neuron could trigger the wavelet transform of the input signal at certain time scales, and encode the spectrum amplitudes into delays between the output fire times and the control spike arriving times. Simulations in this research were conducted using NEural Simulation Tool [15] (NEST) with custom made neuron models.

2.1 Wavelet Encoding Spiking Neuron Model

Although linear summation of synaptic currents and external current has been widely accepted as a simplified relationship among the afferent stimulations in large scale ASNN, the interaction between post-synaptic currents was found to be more complicated in biological nervous system. Koch and Segev [14] found that biological neurons might approximate sum of products among different groups of synaptic currents. Inspired by this finding, we designed a two-stage modulate-and-integrate module, where the multiplication is performed instead of summation between the input signal and synaptic currents. The first stage of the module incorporates the integration of the multiplication of external current and a wavelet shape synaptic current, while the second stage modulate the output from first stage with an exponential decay synaptic current. We will prove that using our preprocessing module together with a LIF neuron, input signal could be decomposed into wavelet spectrum and such spectrum amplitude could be encoded into synchronized spike trains.

In reference to Fig. 1, C_{int} and C_{enc} are delay synchronized clock spikes satisfying:

$$t_i^{\text{enc}} - t_i^{\text{int}} = T_{\text{e}} \tag{1}$$

where T_{e} is the delay phase, t_i^{int} and t_i^{enc} are time of spikes in C_{int} and C_{enc} respectively, with $i = 1, 2, ..., n$ being the index of each spike. The interval of spikes in both C_{int} and C_{enc} is T_{clk}. C_{int} and C_{enc} are converted into post-synaptic current I_{enc} and I_{int} by synapse S_{int} and S_{enc} respectively. Input signal I_{e} is multiplied with I_{int}, and integrated by neuron N_{int} into its state variable v. N_{enc} is a normal LIF neuron, stimulated by the absolute amplitude of v modulated with I_{enc}.

The overall dynamics of this encoding unit could be specified by the following equations:

$$\tau \frac{du(t)}{dt} = -u(t) + \frac{\tau}{C_{\text{m}}} \left| v(t) \right| I_{\text{enc}}(t) \tag{2}$$

$$a \frac{dv(t)}{dt} = I_{\text{e}}(t) I_{\text{int}}(t) \tag{3}$$

where u is the state variable of N_{enc}, I_{enc} and I_{int} are summations of the post-synaptic currents of spikes in C_{enc}, and C_{int} respectively, and are defined as follows:

$$I_{\text{enc}}(t) = \sum_i \exp\left(-\frac{t - t_i^{\text{enc}}}{\tau} \right) \Theta\left(t - t_i^{\text{enc}} \right) \tag{4}$$

$$I_{\text{int}}(t) = \sum_i \sqrt{a} \Psi\left(t - t_i^{\text{int}} - d, \sigma \right) \Theta\left(t - t_i^{\text{int}} \right) \tag{5}$$

where Ψ is a wavelet mother function used as the PSC for S_{int}, with a representing the scale of the wavelet, $\sigma = a\, f_s$ indicating the time scale of the wavelet related to the sampling frequency f_s, d serving as an offset parameter, and Θ being a Heaviside step function. We selected a shifted Mexican-hat wavelet mother function for Ψ as a demonstration here:

$$\Psi(t, \sigma) = \frac{2}{\sqrt{3}\pi^{1/4}} \left(1 - \frac{t^2}{\sigma^2} \right) \exp\left[-\frac{t^2}{2\sigma^2} \right] \tag{6}$$

Assuming that the length of integration period T_{i} satisfies $T_{\text{i}} < T_{\text{clk}}$, we could define $d = T_{\text{i}} / 2$ in (5), so that the wavelet function is centered within each integration window. Note that both I_{enc} and I_{int} are constructed in a unitless manner for the model simplification.

Suppose that each spike in C_{int} could reset the state variable v of neuron N_{int} to zero, and that σ is significantly smaller than T_{clk}, then (2) could be solved for $t_i^{\text{int}} \le t < t_{i+1}^{\text{int}}$ as:

$$v(t) = \frac{1}{\sqrt{a}} \int_{t_i^{\text{int}}}^{t} I_{\text{e}}(\zeta) \Psi(\zeta - t_i^{\text{int}} - T_{\text{i}} / 2, \sigma) d\zeta \tag{7}$$

Suppose further that σ is significantly smaller than T_i, and consider that $\Psi(t,\sigma)\to 0$ when $t>T_i$ or if $t<0$, then (7) could be approximated by:

$$\begin{aligned} v(t) &= \frac{1}{\sqrt{a}}\int_{-\infty}^{\infty} I_\mathrm{e}(\zeta)\Psi\left(\zeta - t_i^\mathrm{int} - T_\mathrm{i}/2, \sigma\right)d\zeta \\ &= X_\mathrm{w}\left(t_i^\mathrm{int} + T_\mathrm{i}/2, \sigma\right) \end{aligned} \tag{8}$$

for $t_i^\mathrm{int} + T_\mathrm{i} \le t < t_{i+1}^\mathrm{int}$, where X_w is the wavelet transform of input I_e at translation $t_i^\mathrm{int} + T_\mathrm{i}/2$ and time scale σ.

Assuming that:

$$T_\mathrm{i} < T_\mathrm{e} < T_\mathrm{clk} \tag{9}$$

and suppose each input spike from C_enc could reset the state variable from u to u_c for neuron N_enc, (2) could be solved for $t_i^\mathrm{enc} \le t < t_{i+1}^\mathrm{enc}$ as:

$$u(\Delta t) = u_\mathrm{c}\exp\left(-\Delta t/\tau\right) + V(\Delta t) \tag{10}$$

$$V(\Delta t) = \frac{\tau\Delta t}{C_\mathrm{m}}\exp\left(-\Delta t/\tau\right)\left|X_\mathrm{w}\left(t_i^\mathrm{int} + T_\mathrm{i}/2, \sigma\right)\right| \tag{11}$$

where Δt is the elapsed time since last input spike from C_enc arrives at the neuron. Note that the absolute value operation applied to v makes $V(\Delta t)$ a function of the absolute spectrum of the wavelet transform X_w. The absolute spectrum is preferable to power spectrum of the wavelet transform, in the sense that it ensures that the units in equation (10) are balanced without need for extra constants.

We considered two different combinations of reset potential u_c and output firing threshold u_th for N_enc:

i) Negative threshold: $u_\mathrm{c} < u_\mathrm{th} < 0$.
ii) Positive threshold: $u_\mathrm{c} = 0$ and $u_\mathrm{th} > 0$.

In the first combination, as long as

$$T_\mathrm{clk} - T_\mathrm{e} > \tau\ln\left(u_\mathrm{th}/u_\mathrm{c}\right) \tag{12}$$

$V(\Delta t)$ is a non-negative function. The membrane potential will exceed the threshold and an output spike will be generated during each time segment $\left[t_i^\mathrm{enc}, t_{i+1}^\mathrm{enc}\right)$. The fire delay T in the i-th segment could be solved from:

$$\left|X_\mathrm{w}\right| = \frac{C_\mathrm{m}}{\tau T}\left[u_\mathrm{th}\exp\left(T/\tau\right) - u_\mathrm{c}\right] \tag{13}$$

where T is guaranteed to be a monotonic decreasing function of $\left|\mathrm{X}_\mathrm{w}\right|$.

For the second combination, consider that $V(\Delta t)$ is a bell shape function which reaches its maximum when $\Delta t = \tau$, the membrane potential could exceed the threshold only if the wavelet spectrum amplitude satisfies:

$$\left|X_\mathrm{w}\right| \ge X_\mathrm{th} = \frac{u_\mathrm{th}C_\mathrm{m}}{\mathrm{e}\tau^2} \tag{14}$$

in which case the firing delay T could be solved from:

$$\left|X_\mathrm{w}\right| = \frac{u_\mathrm{th}C_\mathrm{m}}{\tau T\exp\left(-T/\tau\right)} \tag{15}$$

Note that T is always less than τ in (15), which ensures that T is a monotonic decreasing function of $\left|X_\mathrm{w}\right|$ when the amplitude spectrum $\left|X_\mathrm{w}\right|$ is larger than the threshold X_th. If the wavelet spectrum amplitude is smaller than X_th, the LIF neuron N_enc will not fire during $\left[t_i^\mathrm{enc}, t_{i+1}^\mathrm{enc}\right)$.

In both combinations discussed above, the wavelet spectrum of input signal I_e is encoded into delay phase T which is the difference between the time of each output fire and the arrival time of the most recent input spike in C_enc. Thus, larger wavelet spectrum amplitude corresponds to faster firing after each clock spike.

2.2 Encoding Implementation

Synapses and neurons as described in (2) through (6) are implemented in NEST with a single customized neuron model referred to as the Wavelet Sensor Neuron (WSN). In order to balance the accuracy and efficiency while solving ODEs for WSN, exponential integration method has been adopted to solve the state variable u, and Simpson's rule was applied to the integration for state variable v:

$$u_{n+1} = P_{32}s_n\left|v_n\right| + P_{33}u_n \tag{16}$$

$$v_{n+1} = \frac{h}{6}\left(I_\mathrm{m}(t_n) + 4I_\mathrm{m}\left(t_n + \frac{h}{2}\right) + I_\mathrm{m}\left(t_n + h\right)\right) + v_n \tag{17}$$

$$s_{n+1} = P_{33}s_n \tag{18}$$

$$I_\mathrm{m}(t) = P_2\left(1 - \frac{\delta t^2}{\sigma^2}\right)\exp\left(-\frac{\delta t^2}{2\sigma^2}\right)I_e(t) \tag{19}$$

$$\delta t = t - T_\mathrm{i}/2 - t^\mathrm{int} \tag{20}$$

where subscript n indicates the n-th simulation step, h is the simulation step size, t^int is the arrival time of the most recent spike in C_int, and P_2, P_{32}, and P_{33} are constant parameters defined by the following relations:

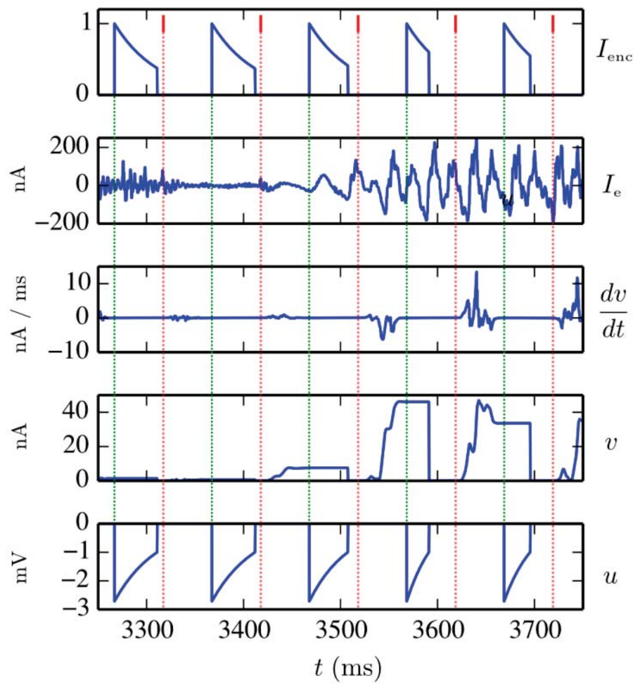

Fig. 2 Time course of variables in one WSN with $\sigma = 5.64$ ms. Red vertical dash lines indicates the arrival times of spikes in C_{int}; green dash lines indicates the arrival times of spikes in C_{enc}.

$$\begin{aligned} P_2 &= \frac{2}{\sqrt{3a}\pi^{1/4}} \\ P_{32} &= \frac{\tau}{C_m}\left[1-\exp\left(-h/\tau\right)\right] \\ P_{33} &= \exp\left(-h/\tau\right) \end{aligned} \tag{21}$$

The WSN model incorporates two types of spike receptors to distinguish whether a spike is send to S_{int} or S_{enc}, in the same manner as any other neuron model implemented in NEST which could receive spike input from more than one type of synapses. Input spikes with receptor type I are recognized as spikes sent to S_{int}, which could reset v_n to zero and set t^{int} to the current time; while input spikes with receptor type II are recognized as spikes sent to S_{enc}, which in turn could reset u to u_c and s to zero.

A normal LIF neuron N_{clk} with an exponential decay synapse is implemented in this network as the clock generator. This LIF neuron is connected to itself with axon delay T_{clk} and synaptic efficacy large enough to generate a new output spike from itself. A short strong pulse injected to N_{clk} could initialize the first firing of N_{clk}, and generate oscillatory clock spikes at constant interval approximate to T_{clk}. These clock spikes are sent to type I receptors of WSN neurons with a short delay D_0, and type II receptors with a longer delay T_e.

We built an encoding network to convert the human voice records obtained from Census Database of Carnegie Mellon University [16] (AN4) into spike trains related to the wavelet spectrum. An array of 100 WSNs with $\tau = 45$ ms and σ varies between 0.2 ms and 10.0 ms were implemented in the encoding network. The spike trains could encode frequency components ranging from 100 Hz to 50 kHz in the input signal, which is wider than the human voice frequency limitations. Time constants $T_{\text{clk}} = 100$ ms, $D_0 = 1.0$ ms, $T_i = 45$ ms, and $T_e = 50$ ms was selected to meet all the requirements posed by (9). A negative threshold $V_{\text{th}} = -1.0$ mV was used in this implementation. The reset membrane voltage was set to $u_c = -2.72$ mV so that the longest spike delay is $T_{\max} = 45$ ms, according to the solution of (10) with $V(T) = 0$ mV and $u(T_{\max}) = u_{\text{th}}$. Since $T_e + T_{\max} < T_{\text{clk}}$, there is always one output spike from each WSN within one clock cycle.

3 Results and Discussion

The record file "an253-fash-b.raw" from the training set of AN4 database was used as the input to the WSN encoding network. The state variables of each WSN neurons were recorded for the testing purpose. A portion of the recorded variables of one WSN with $\sigma = 5.64$ ms was captured and plotted in Fig. 2

Vertical red dash lines in Fig. 2 represent the arrival times of the clock spikes for the type I synapse receptor of this neuron. Input I_e was modulated with the wavelet kernel for 45 ms after each clock signal. When I_e contains components matching the 5.64 ms time scale of the wavelet function, the WSN generates a larger modulated current, yielding as a consequence a larger state variable v. The clock spikes arrive at the type II synapse receptor of this WSN after 50 ms delay (indicated by the green vertical lines in Fig. 2, which trigger the encoding periods. At the beginning of each encoding period, the integration of v has already finished, thus v holds its value for the whole encoding period. The LIF neuron

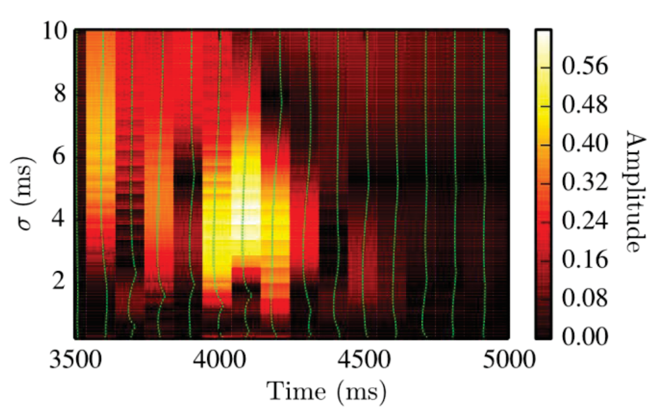

Fig. 3 Comparison of WSN encoding with Continuous Wavelet Transform at corresponding translations. Green lines bars output spikes from the WSN array

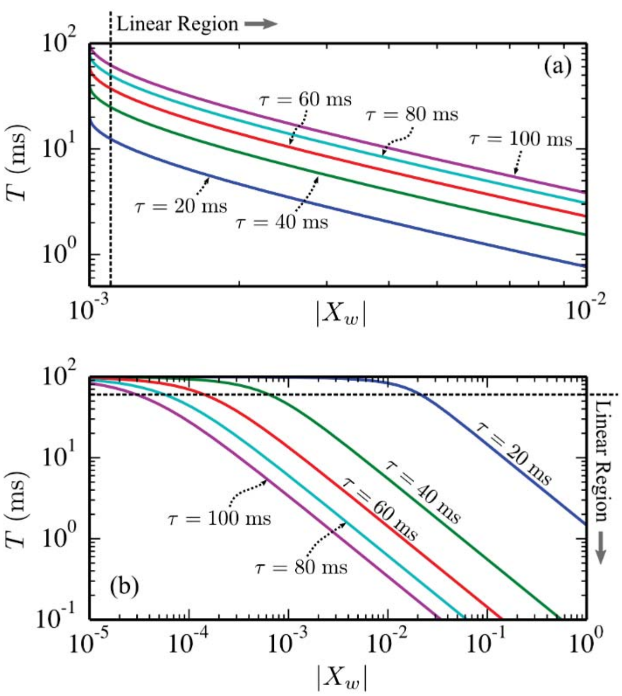

Fig. 4 Logarithm relationship of the input intensity and output spike delay: (a) the relationship of positive threshold WSNs; (b) the relationship of negative threshold WSNs.

incorporated by the WSN would encode the constant v into an output firing delay. It could be found from the records of u that, the WSN fires faster when the input signal I_e contains components matching $\sigma = 5.64$ ms (i.e., periods from 3520 ms to 3720 ms), yet fires slower at almost the end of each encoding period when I_e contains only higher frequency components (i.e., periods from 3120 ms to 3320 ms).

The voice record used in this experiment was the sound of female pronouncing the word "GO". The output spikes of all 100 WSNs were raster-plotted for the time range from 3500 ms to 5000 ms using short vertical green bars as shown in Fig. 3. Continuous wavelet transform using Mexican-hat wavelet was also applied to the same voice record. The wavelet transform at translations $t_i^{clk} + 22.5$ ms were color coded and superimposed on Fig. 3, where t_i^{clk} are the firing times of N_{clk}. It could be found from Fig. 3 that, the change of the fundamental frequency when pronouncing the word "GO" was clearly captured by the Mexican-hat wavelet transform, and the delay phases of WSN output fires were a good representation of the wavelet spectrum amplitudes during each clock cycle. Such phase encoded spike trains are applicable to any supervised spiking neural learning. Thus, the clustered or classified features of the frequency changes could be used to recognize the word pronounced. The phase delays of the WSN array in this example could substitute for the spectrogram in estimating key characteristics in speech recognition [17], and could support the building of speech perception system using ASNN.

3.1 Encoding Non-linearity

The logarithm relationship between stimulation intensity and the delay phase of encoded spikes in sensory neurons was identified by many neurologists [18]. In many spiking neural network applications which implements PE as the sensing method, a log function was applied to the input signals to mimic the logarithm relationship [9], [12]. The WSN encoding method is highly nonlinear according to (13) and (15), yet the logarithmic relationship between stimulation intensity and the delay phase of spikes is a natural feature of the WSN encoding.

As shown in Fig. 4, the linearity between $\log(|X_w|)$ and $\log(T)$ could be found in certain regions for the five selected WSN neurons with time constants τ being 20 ms, 40 ms, 60 ms, 80 ms and 100 ms, respectively. In Fig. 4(a), positive firing threshold was adopted for these neurons, and the wavelet spectrum amplitude threshold was set to $X_{th} = 10^{-3}$ for all five neurons. The firing threshold u_{th} for these neurons could be calculated by (14). We could find that WSN could encode $\log(|X_w|)$ to $\log(T)$ in a linear way when $|X_w|$ is in the linear region shown in Fig. 4(a). Different time constants τ introduce different offsets to the linear relationship along the y-axis: larger τ values corresponds to better encoding resolution for small $|X_w|$.

As a comparison, negative firing threshold were used for the WSN neurons in Fig. 4(b), with u_{th} all set to −0.2 mV. u_c for these neurons was adjusted according to:

$$u_c = u_{th} \exp(\tau_{max} / \tau) \qquad (22)$$

such that the maximum output fire delay was always $T_{max} = 100$ ms. Linearity could also be found in the linear region indicated in Fig. 4(b), when T is a bit smaller than T_{max}. Different time constants τ introduce different offsets to the linear relationship along the x-axis.

It should be noted that, using the same τ settings, negative firing thresholds provide better logarithm linearity than positive firing thresholds for the encoding of signals with a larger range of $|X_w|$. Since the parameter τ in the WSN neuron is limited by the encoding window length, negative firing thresholds could be a better choice when the encoding linearity is of interest, as demonstrated in this paper when encoding was performed on the example of the human voice record. However, the $|X_w|$ cut-off feature provided by the positive firing thresholds could be useful when only large values of $|X_w|$ are of interest. The threshold configuration as well as the time constant τ should thus be carefully selected for a given application, so that the features of interest in the input signal could be best encoded into the delay of output fires.

3.2 Mother Wavelet Functions

Although a shifted Mexican-hat wavelet mother function was used for the post-synaptic current shape function in S_{int}, it is not required for the WSN neuron to work properly. Any types of wavelet mother functions could be used as the current shape function in WSN, and the input signal will be decomposed according to the mother wavelet functions selected. If a discrete wavelet is demanded, the kernel function of the discrete wavelet at different time scale with proper shifting should be used as Ψ in (5).

More interestingly, since the integration of the wavelet kernel performs only in a limited time duration, the only requirement for $\Psi(t)$ is that:

$$\lim_{t \to \pm\infty} \Psi(t) = 0 \tag{23}$$

and $\Psi(t)$ is not required to be absolutely integrable and square integrable from $-\infty$ to $+\infty$. Some functions, such as the alpha function:

$$\Psi_{\alpha}(t,\sigma) = \frac{t}{\sigma} \exp\left(-\frac{t}{\sigma}\right) \tag{24}$$

could also be used to decompose the input signals.

3.3 Temporal Resolution

Since the wavelet of a WSN is convolved with the input signal only once during each clock cycle, the encoding temporal resolution of one WSN is limited to the clock interval T_{clk}. Considering that the total of integration time T_{i} and that encoding time T_{e} should be smaller than T_{clk}, and the time constant τ should also be smaller than T_{i}, although a decreased T_{clk} could enhance the encoding temporal resolution, it might also harm the encoding range of the wavelet spectrum amplitude. In order to enhance the temporal resolution of a WSN array without interfering with the encoding range, we could still implement multiple WSNs for each time scale selection, but with different D_0 values. Accordingly, the wavelet transform would be performed at different translations within each clock cycle, and thus could significantly enhance the temporal resolution of the encoding without shrinking the length of each clock cycle.

4 Conclusion and Future Work

Encoding of analog signals into spike trains is one of the most important steps for information processing in biological nervous systems. The encoding method we proposed in this paper incorporates the concepts of synaptic current modulation with phase encoding representation. We proved that the proposed WSN model combining a preprocessing unit and a LIF neuron could perform the wavelet decomposition of the input signal, and convert the wavelet spectrum amplitude at certain translation and time scales into the output fire delay of the WSN neuron.

Encoding networks using WSN neurons were implemented in this study to encode an example of a human voice record, with results that are quite similar to continuous wavelet decomposition. The linearity property and limitations of mother wavelet functions of this WSN encoding method were discussed as a guidance for choosing proper parameters for the WSN network to fit a specific application. We also provide a simple method to overcome the temporal resolution limitation posed by the clock signal, so that the wavelet decomposition could be performed with higher temporal accuracy if needed.

Beyond the above contributions, this work also provides an intuitive insight of how stimulations gathered by sensor neurons might be represented and processed by a biological nervous system: the modulation behavior found between dendrites together with the integration feature of a biological neuron could perform decomposition of stimulation signals similar to wavelet transforms, and encode only those features of interest in the stimulation into the spike delay phases.

There are other possibilities for using the proposed encoding method such as: (1) apply graph theory [19] to find the connectivity between encoded spike trains, or (2) build spiking self-organizing-map and supervised learning systems to further process the encoded spike trains, and classify the patterns represented by the encoded spike trains into meaningful symbols. Although the WSN and the encoding network was implemented in the NEST environment, which is based on a digital computing platform, the concepts of WSN is fully compatible with analog computing. We are interested in developing analog circuits to implement WSN encoding network, so that Ultra Large Scale Integration methods could be used to build a highly parallel neuromorphic system.

5 Acknowledgment

The authors are extremely grateful for the support provided by the National Science Foundation under grants CNS-0959985, CNS-1042341, HRD-0833093, IIP-1338922, and CNS-1429345. The generous support of the Ware Foundation is also greatly appreciated.

6 References

[1] S. Panzeri, R. S. Petersen, S. R. Schultz, M. Lebedev, and M. E. Diamond, "The role of spike timing in the coding of stimulus location in rat somatosensory cortex," *Neuron*, vol. 29, no. 3, pp. 769–777, Mar. 2001.

[2] R. S. Johansson and I. Birznieks, "First spikes in ensembles of human tactile afferents code complex spatial fingertip events.," *Nat. Neurosci.*, vol. 7, no. 2, pp. 170–177, Feb. 2004.

[3] H. Sprekeler, C. Michaelis, and L. Wiskott, "Slowness: an objective for spike-timing-dependent plasticity?," *PLoS Comput. Biol.*, vol. 3, no. 6, pp. 1136–1148, Jun. 2007.

[4] R. R. Keer, A. N. Burkitt, D. A. Thomas, M. Gilson, and D. B. Grayden, "Delay Selection by Spike-Timing-Dependent Plasticity in Recurrent Networks of Spiking Neurons Receiving Oscillatory Inputs," *PLoS Comput. Biol.*, vol. 9, no. 2, p. e1002897, Feb. 2013.

[5] H. De Garis, M. Korkin, F. Gers, E. Nawa, and M. Hough, "Building an artificial brain using an FPGA based CAM-Brain Machine," *Appl. Math. Comput.*, vol. 111, no. 2–3, pp. 163–192, May 2000.

[6] B. Schrauwen and J. Van Campenhout, "BSA, a fast and accurate spike train encoding scheme," in *Proceedings of the International Joint Conference on Neural Networks*, 2003, vol. 4, pp. 2825–2830.

[7] N. Nuntalid, K. Dhoble, and N. Kasabov, "EEG Classification with BSA Spike Encoding Algorithm and Evolving Probabilistic Spiking Neural Network," in *International Conference on Neural Information Processing*, 2011, vol. 7062, pp. 451–460.

[8] Y. Chen, J. Hu, N. K. Kasabov, Z. Hou, and L. Cheng, "NeuCubeRehab: A Pilot Study for EEG Classification in Rehabilitation Practice Based on Spiking Neural Networks," in *International Conference on Neural Information Processing*, 2013, pp. 70–77.

[9] N. Kasabov, K. Dhoble, N. Nuntalid, and G. Indiveri, "Dynamic evolving spiking neural networks for on-line spatio- and spectro-temporal pattern recognition," *Neural Networks*, vol. 41, no. Special Issue, pp. 188–201, May 2013.

[10] S. Ghosh-Dastidar and H. Adeli, "Improved spiking neural networks for EEG classification and epilepsy and seizure detection," *Integr. Comput. Aided. Eng.*, vol. 14, no. 3, pp. 187–212, Aug. 2007.

[11] S. G. Wysoski, L. Benuskova, and N. K. Kasabov, "Evolving spiking neural networks for audiovisual information processing," *Neural Networks*, vol. 23, no. 7, pp. 819–835, Sep. 2010.

[12] J. A. Wall, L. J. McDaid, L. P. Maguire, and T. M. McGinnity, "Spiking neural network model of sound localization using the interaural intensity difference," *IEEE Trans. Neural Networks Learn. Syst.*, vol. 23, no. 4, pp. 574–586, Apr. 2012.

[13] T. Rumbell, S. L. Denham, and T. Wennekers, "A spiking self-organizing map combining STDP, oscillations, and continuous learning," *IEEE Trans. Neural Networks Learn. Syst.*, vol. 25, no. 5, pp. 894–907, May 2014.

[14] C. Koch and I. Segev, "The role of single neurons in information processing.," *Nat. Neurosci.*, vol. 3, pp. 1171–1177, Nov. 2000.

[15] M.-O. Gewaltig and M. Diesmann, "NEST (NEural Simulation Tool)," *Scholarpedia*, vol. 2, no. 4, p. 1430, Apr. 2007.

[16] J. Kominek and A. W. Black, "The CMU Arctic Speech Databases," in *ISCA Speech Synthesis Workshop*, 2004, pp. 223–224.

[17] P. Gómez-Vilda, J. M. Ferrández-Vicente, and V. Rodellar-Biarge, "Simulating the phonological auditory cortex from vowel representation spaces to categories," *Neurocomputing*, vol. 114, pp. 63–75, Aug. 2013.

[18] T. J. Sejnowski, "Time for a New Neural Code?," *Nature*, vol. 376, no. 6, pp. 21–22, Jul. 1995.

[19] S. Sargolzaei, M. Cabrerizo, M. Goryawala, A. S. Eddin, and M. Adjouadi, "Functional Connectivity Network based on Graph Analysis of Scalp EEG for Epileptic Classification," in *Signal Processing in Medicine and Biology Symposium*, 2013, pp. 1 – 4.